Predictive subpixel spatial/spectral modeling using fused HSI and MSI data

F. A. Kruse[**]
Horizon GeoImaging, LLC
4845 Pearl East Circle, Suite 101, Boulder, CC USA 80301-6113

ABSTRACT

Hyperspectral Imagery (HSI) data are inherently more expensive and difficult to acquire than Multispectral Imagery (MSI) data. Most HSI acquisitions are currently limited to relatively low spatial resolution with the inherent limitation that they are not able to spatially resolve many important targets. Higher spatial resolution MSI data are available, however, they typically don't provide sufficient spectral resolution to allow unambiguous identification of specific targets. We describe a new method using predictive modeling of combined HSI/MSI data to generate simulated high-spatial-resolution, high-spectral-resolution image data. Targets observed by the low spatial resolution HSI sensor are spectrally resolved through linear spectral unmixing, but not spatially resolved. Targets observed by higher spatial resolution MSI sensor are partially spatially resolved but lower spectral resolution doesn't allow target identification. The fused data are used to predict the subpixel locations of HSI-identified subpixel targets within the superior MSI spatial resolution. Comparison of individual HSI endmember spectra to MSI signatures at multiple MSI pixels allows mapping the spatial locations of specific HSI endmembers creating a simulated HSI dataset that allows location of spectrally resolved targets. The combined data incorporate the best features of HSI/MSI to allow improved target detection and characterization.

Keywords: subpixel modeling, spectral mixing, spatial-spectral modeling, HSI-MSI data fusion

1. INTRODUCTION

Using information from higher resolution images to sharpen lower resolution images is commonly accomplished using statistical approaches such as principal components or various color spaces [1, 2]. More recently, attempts have been made to use the physical properties of coincident datasets to construct composite higher-resolution images [3, 4]. These approaches, however, are still generally focused on producing visually interpretable images or datasets. Researchers have typically found it difficult to simultaneously preserve the HSI spectral integrity and the MSI spatial resolution.

The research described here takes a different approach by attempting to assign specific spectral signatures to pixel targets based on spectral mixture analysis. Spectral endmembers and spatial mixing were examined in both HSI and MSI data and predictive modeling of the combined datasets was used to generate simulated high-spatial-resolution, high-spectral-resolution image data that allow determination of subpixel locations and characteristics of specific target materials. Hyperspectral data were used as the basis for spectral mapping by extraction of key spectral signatures using linear spectral unmixing and convex geometry approaches [5, 6]. Unfortunately, many targets of interest occur at subpixel resolution in typical HSI data, however, fortunately, experience indicates that we can still resolve these targets spectrally (non-literally), even though their spatial occurrence isn't apparent in the HSI data [7, 8]. This research takes advantage of coincident higher spatial resolution MSI data by matching MSI/HSI signatures to allow determination of the spatial locations of specific spectral signatures within the larger HSI pixel and generation of simulated high-spatial-resolution HSI data. This approach allows improved detection, characterization, identification, and mapping of prospective subpixel targets.

[**] kruse@hgimaging.com; phone 303-499-9471; fax 303-499-2887; http://www.hgimaging.com

2. APPROACH AND METHODS

2.1. General

This approach to analysis of the combined MSI/HSI data requires that the data be radiometrically calibrated, atmospherically corrected to reflectance, and spatially coregistered at the MSI spatial resolution. The MSI data must have significantly better spatial resolution than the HSI data. Given these data conditions, we determine spectral endmembers using the HSI data, use the MSI sensor model (band passes) to resample the HSI endmembers to match the MSI spectral resolution, and perform spectral matching to the MSI data to assign a predominant endmember to each MSI pixel and create a simulated high-spatial-resolution dataset. Figure 1 schematically illustrates the concept.

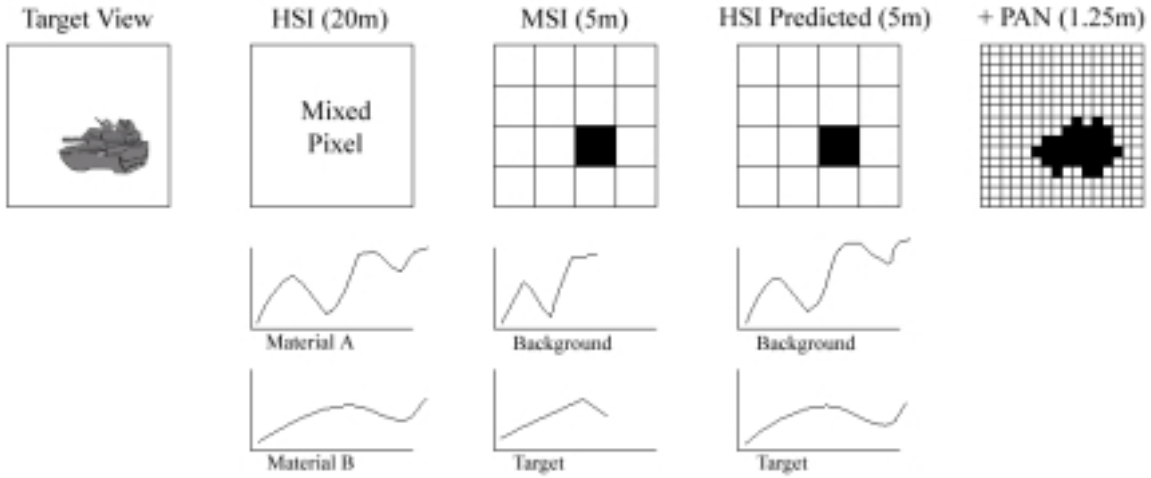

Figure 1: Schematic (simplified) view of HSI simulation modeling concept. Target (left panel) observed by low spatial resolution HSI sensor is spectrally resolved through linear spectral unmixing, but not spatially resolved (2nd panel from left). Target observed by higher spatial resolution MSI sensor is partially spatially resolved but lower spectral resolution doesn't allow target identification (center panel). Simulated HSI dataset allows location of spectrally resolved target (2nd panel from right). Combination with higher spatial resolution Panchromatic data potentially further resolves the spatial target and identification is made from HSI spectral signature (right panel).

2.2. Calibrate/Atmospherically Correct Data

All datasets are radiometrically calibrated using sensor calibration information (or acquired in calibrated form from the data providers). Further correction of the data to reflectance using atmospheric models is required. We used the commercially available MODTRAN-based "ACORN" software [9] to atmospherically correct both the HSI and MSI data to provide consistent basis for spectral comparison and matching. Where possible, data are further corrected using ground spectral measurements collected at the time of data acquisition using a field spectrometer to insure the best atmospheric correction. Additionally, empirical corrections using linear regression between HSI and MSI datasets for known targets are used where necessary to refine the corrections.

2.3. Coregister Datasets

Lower spatial resolution HSI data are co-registered with higher spatial resolution MSI data using nearest neighbor resampling to produce an HSI data set at MSI spatial resolution (resulting HSI data are spatially oversampled – no new spatial information will be introduced to HSI data). Ground Control Points (GCPs) selected in the MSI data and verified using maps and field reconnaissance are matched with corresponding HSI pixel locations and used to perform the geometric corrections. The nearest neighbor resampling is used to minimize resampling effects. GCPs are also used to assist with verification of target locations.

2.4. Analyze HSI data

Hyperspectral data are used to determine spectral endmembers at the subpixel level using standardized HSI subpixel mapping techniques [5, 6, 8] (Figure 2),

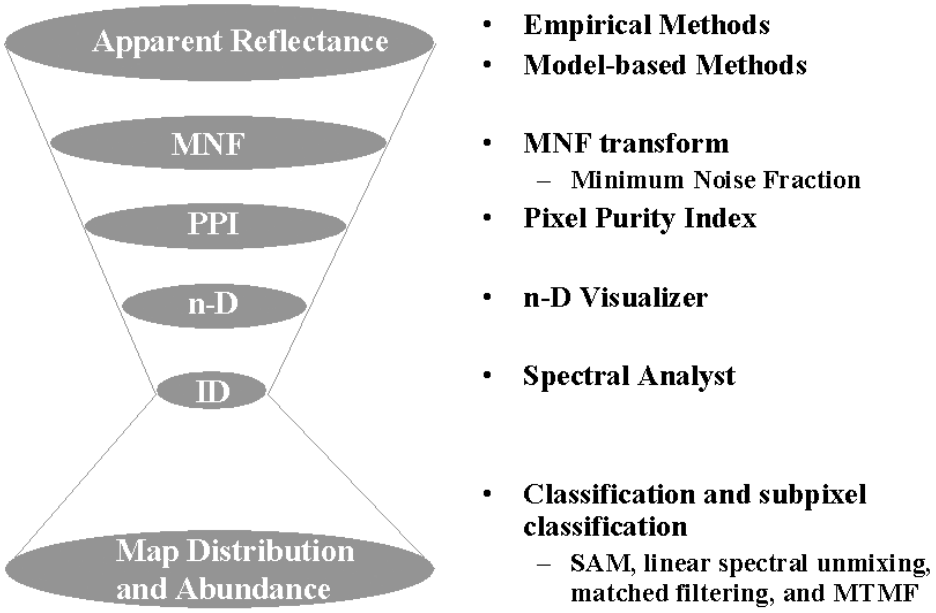

Figure 2: Standardized hyperspectral analysis scheme. Note the "hourglass" shape, which schematically represents the reduction of the hyperspectral data to just a few key spectra at the "neck" and then expansion back to spectral maps of the full dataset.

These methods were developed by Analytical Imaging and Geophysics, LLC (AIG) while the author was associated with that company. They also are implemented and documented within the "Environment for Visualizing Images" (ENVI) software system originally developed by AIG scientists (now a Research Systems Inc [RSI] commercial-off-the-shelf [COTS] product) [10]. They are also described briefly below. This is not the only way to analyze these data, but we have found that it provides a consistent way to extract spectral information from hyperspectral data without *a priori* knowledge or requiring ground observations [6]. The analysis approach consists of the following steps:

1. correction for atmospheric effects using an atmospheric model "ACORN" [9].
2. spectral compression, noise suppression, and dimensionality reduction using the Minimum Noise Fraction (MNF) transformation [8].
3. determination of endmembers using geometric methods (Pixel Purity Index – "PPI") [8].
4. extraction of endmember spectra using n-dimensional scatter plotting [8].
5. identification of endmember spectra using visual inspection, automated identification, and spectral library comparisons [11].
6. production of endmember maps using a variety of mapping methods. The Spectral Angle Mapper (SAM) algorithm [12] is used as a first-cut mapping method. The preferred mapping method "Mixture-Tuned-Matched-Filtering" (MTMF) provides more precise results and is basically a partial linear spectral unmixing procedure, producing abundance information for each endmember [13].

2.5. Model HSI/MSI Data

MSI data are resampled to the HSI wavelengths prior to mapping to produce spectra with the same spectral band spacing over a shared wavelength range (MSI need not cover full HSI spectral range). Resulting resampled MSI data are spectrally oversampled - no new spectral information is introduced to MSI data. Alternatively, HSI endmember spectra are resampled to MSI band spacing using known instrument response curves for each spectral band.

2.6. Match HSI and MSI Pixel Spectra

After resampling, multiple MSI spectra are extracted corresponding to each pixel of HSI data and compared to HSI endmembers using various spectral matching methods (eg: Spectral Angle Mapper (SAM) [12], linear spectral unmixing[5], and/or Mixture-Tuned Matched-Filtering (MTMF)[13]. Best match an HSI endmember spectra are assigned to corresponding MSI spatial locations (substituted for MSI spectra) in the MSI dataset to form a predictive model of HSI data at higher MSI resolution. MSI pixels that don't match HSI specific endmember – or satisfy a specified "purity" threshold retain their oversampled MSI signatures (or can be mapped to null pixels rather than being mapped to a specific HSI spectrum).

2.7. Accuracy Assessment

Though beyond the scope of this initial proof-of-concept investigation, future accuracy assessment will consist of evaluation of pixel signatures and location accuracy for subpixel mapping using higher spatial resolution HSI data as well as field spectral measurements.

3. EXAMPLE USING SIMULATED DATA

A simulated nested HSI and MSI data set was created using Airborne Visible/Infrared Imaging Spectrometer [14, 15] (AVIRIS) endmember spectra (224 spectral bands) extracted from an urban scene. Five endmembers were selected, 1. dry grass, 2. asphalt, 3. green vegetation, 4. roofing material, and 5. exposed rock (Figure 3). The endmember spectra were linearly mixed in the proportions 75% dry grass, and 6.25% each of the other endmembers to form a uniform mixed signature in the simulated HSI dataset (Figure 3). The resulting HSI dataset consists of a single pixel having one spectral signature (Figure 3 - right). A corresponding MSI dataset (using 25 MODIS/ASTER Airborne Simulator [MASTER] bands)[16] was constructed at higher spatial resolution (4 x 4 pixels covering the same area). The specific endmembers (resampled to MASTER spectral resolution and band passes) were assigned to MSI pixels covering the appropriate proportional area corresponding to that used for the simulated mixed HSI signature - 75% dry grass, and 6.25% each of the other endmembers (Figure 4).

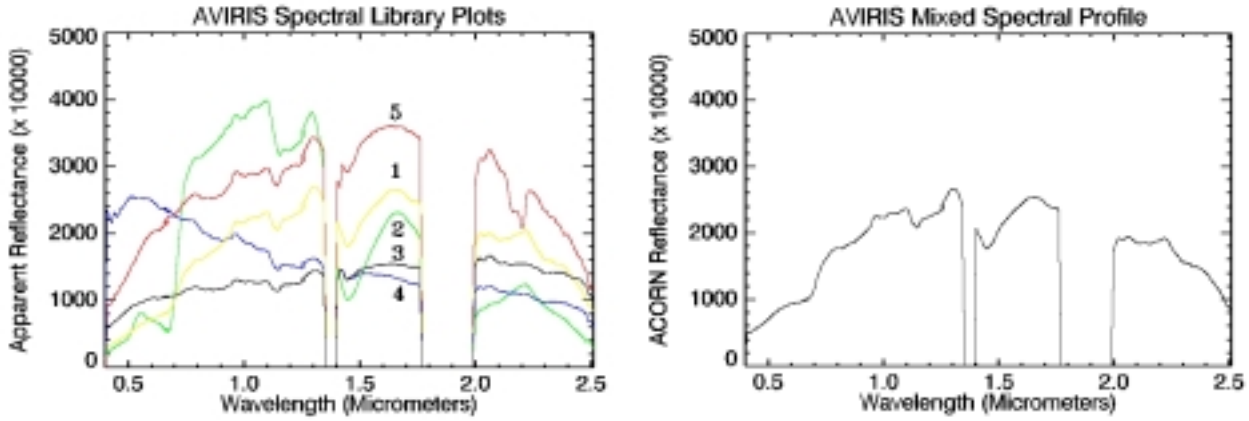

Figure 3: AVIRIS-extracted endmember spectra (left). Yellow (1) is dry grass, green (2) is green vegetation, black (3) is asphalt, blue (4) is roof, and red (5) is rock and red (5). Mixed spectrum shown on right.

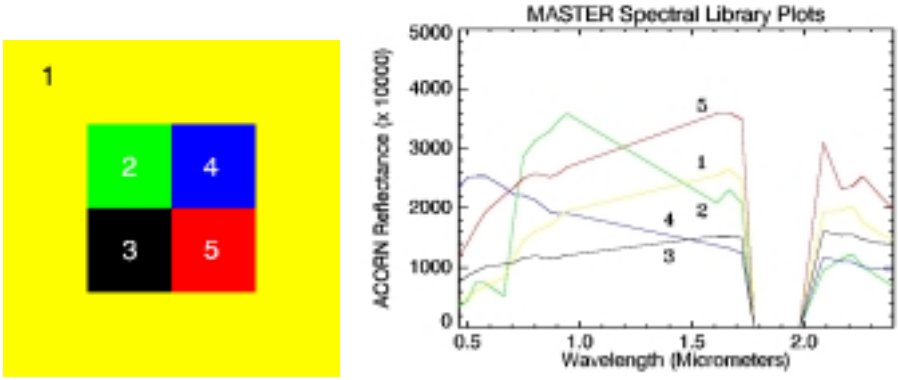

Figure 4. Pixel mask (left) showing distribution of specific endmembers in the simulated MSI data set (colors as for Figure 3 [left]). Yellow (1) is dry grass, green (2) is green vegetation, black (3) is asphalt, blue (4) is roof, and red (5) is rock and red (5). MSI-resampled endmember spectra (right) at MASTER spectral resolution and band basses.

Next, the AVIRIS endmembers were matched to the MSI endmembers using spectral unmixing and their spatial distributions were mapped (Figure 5). As expected, the MSI data now illustrate the distribution of the HSI spectral endmembers incorporated in the single mixed HSI spectral signature at the higher MSI spatial resolution. The simulated high-spatial resolution HSI dataset is created by substituting the appropriate AVIRIS spectral signature into the mapped MSI pixel. While this might seem like a self-evident exercise that just verifies what you already know about the data, it is useful as an illustration of how the MSI-HSI prediction model should work for locating the spatial distribution of specific HSI endmembers in a MSI dataset (albeit under simplified conditions).

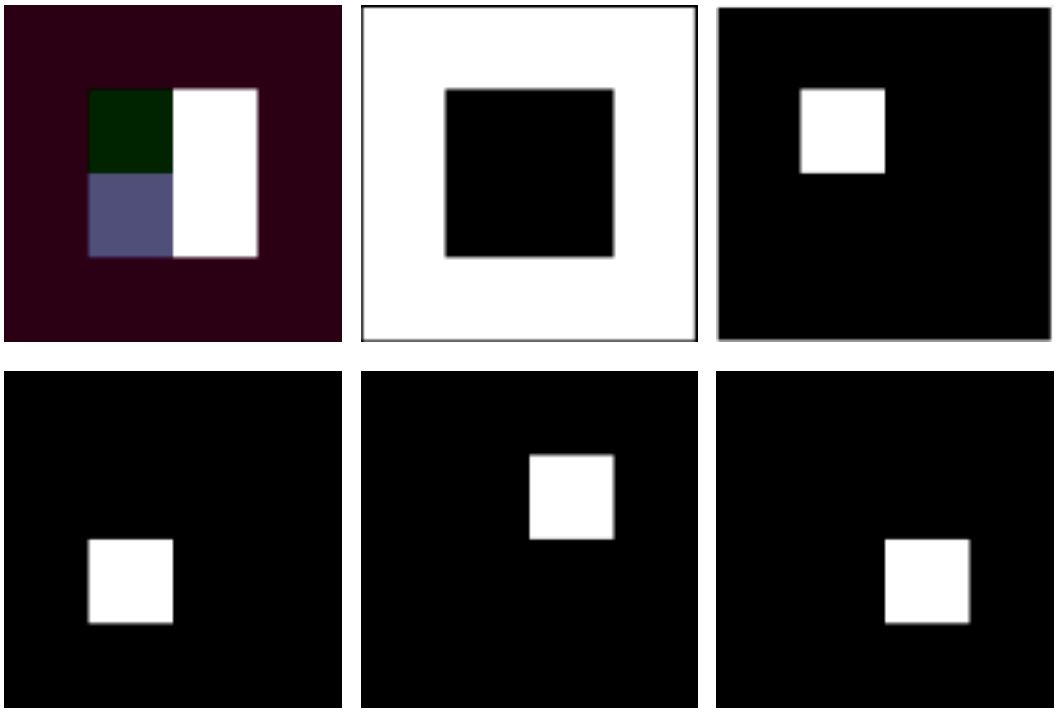

Figure 5. MSI spectral unmixing results. Simulated true color composite image (top left) and unmixing results (predominant endmember coded as white) for dry vegetation (top center), green vegetation (top right), asphalt (bottom left), roofing material (bottom center), and rock (bottom right).

4. AVIRIS and MASTER Data Demonstration

The concepts described above were tested using approximately 20m spatial resolution AVIRIS data acquired 30 September 1999 and approximately 5m spatial resolution MASTER data acquired 21 September 1999 for an area covering portions of the city of Golden, Colorado. AVIRIS is an imaging spectrometer covering the 0.4 – 2.5 micrometer range in 224 bands with approximately 10 nanometer full-width-half-max (FWHM) for all bands [14, 15]. MASTER is a multispectral scanner with 50 bands spanning the 0.4 – 13 micrometer range with approximately 40 to 70 nanometer (variable per band) FWHM [16]. For analyses, both the AVIRIS and MASTER data were corrected to apparent reflectance using the ACORN software [9] and appropriate parameters reflecting location, acquisition dates and times, flight altitudes, and terrain elevation. Excluding atmospheric absorption bands, 176 AVIRIS bands were used and 20 of the 25 MASTER VNIR-SWIR bands were used (both covering the 0.4 – 2.5 micrometer range). To obtain an improved reflectance match, MASTER apparent reflectance data were then adjusted to more closely match the AVIRIS data using the empirical line method [17]. (Gains and offsets were determined that match reflectance for selected targets in the MASTER data to their corresponding targets in the AVIRIS data.) Spectral analysis was performed on the reflectance-corrected data at the original spatial resolutions. For purposes of comparison, AVIRIS and MASTER true-color images were then map-registered using selection of ground control points (GCPs) on corresponding Quickbird orthorectified 2.4m multispectral imagery and using Delaunay Triangulation, and nearest neighbor resampling (Figure 6).

Figure 6: AVIRIS geocorrected true color image (left) and MASTER geocorrected image (right).

The AVIRIS data were analyzed using the n-Dimensional procedures described above and HSI endmembers were extracted (Figure 7, Left). The MASTER spectral responses for the closest calibration date (June 1999) were used to resample the AVIRIS endmember spectra to MASTER wavelengths and band responses (Figure 7, Right).

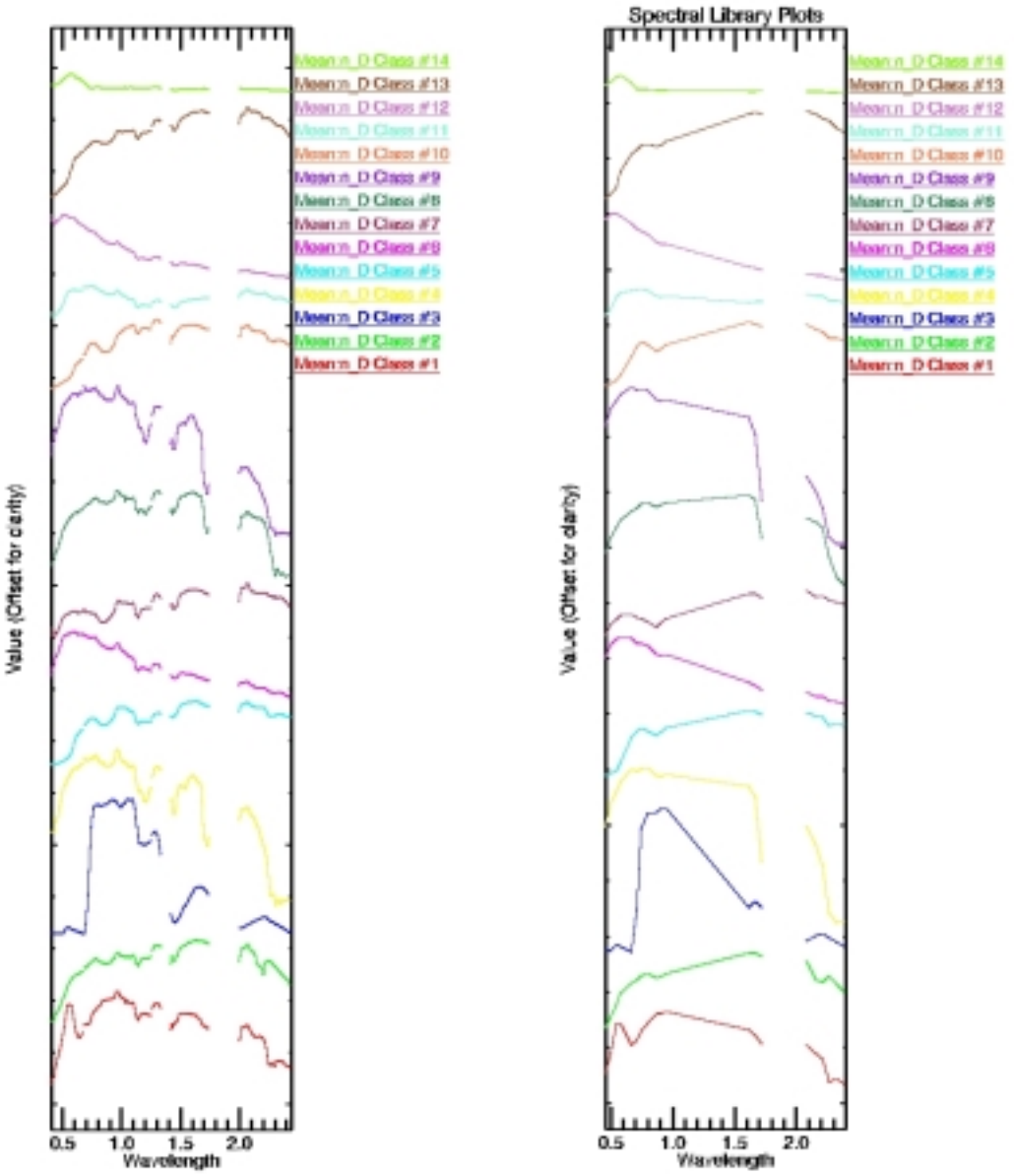

Figure 7: AVIRIS endmember spectra (left) and modeled MASTER spectra (right) created by resampling the AVIRIS spectra using the MASTER spectral band responses. Spectra are offset for clarity. Several of the materials represented by the AVIRIS spectra can be identified by inspection, including #2 (kaolinite with iron-oxides), #3 (green vegetation); #5 (Red Tile Roofs); #10, and #13 (iron-oxide-rich surfaces); and #14 (water). Other AVIRIS spectra require field verification to determine exact materials.

Both the Spectral Angle Mapper (SAM) and Mixture-Tuned-Matched-Filtering (MTMF) were then used to map the spatial locations of the predominant endmembers on both the AVIRIS and MASTER data. Analysis results (classification images) were geocorrected to match the corrected true color images for reference (Figures 8 and 9).

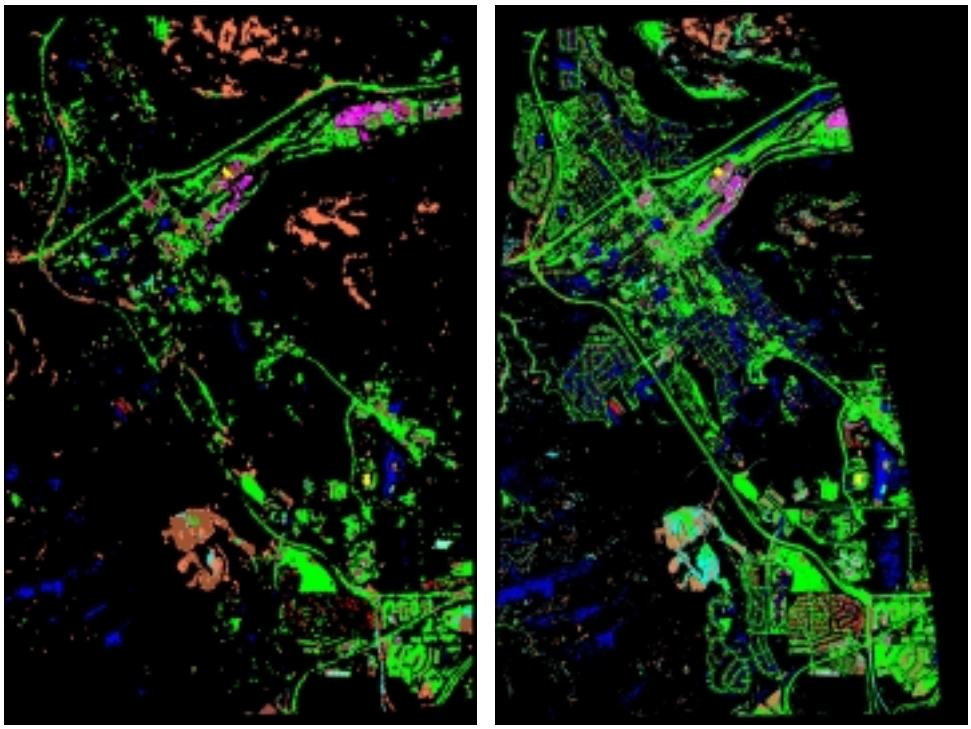

Figure 8: AVIRIS (Left) and MASTER (Right) SAM mapping results showing predominant material for each pixel for the Golden Colorado AVIRIS and MASTER data. Classification colors match the colors for endmembers shown in Figure 7.

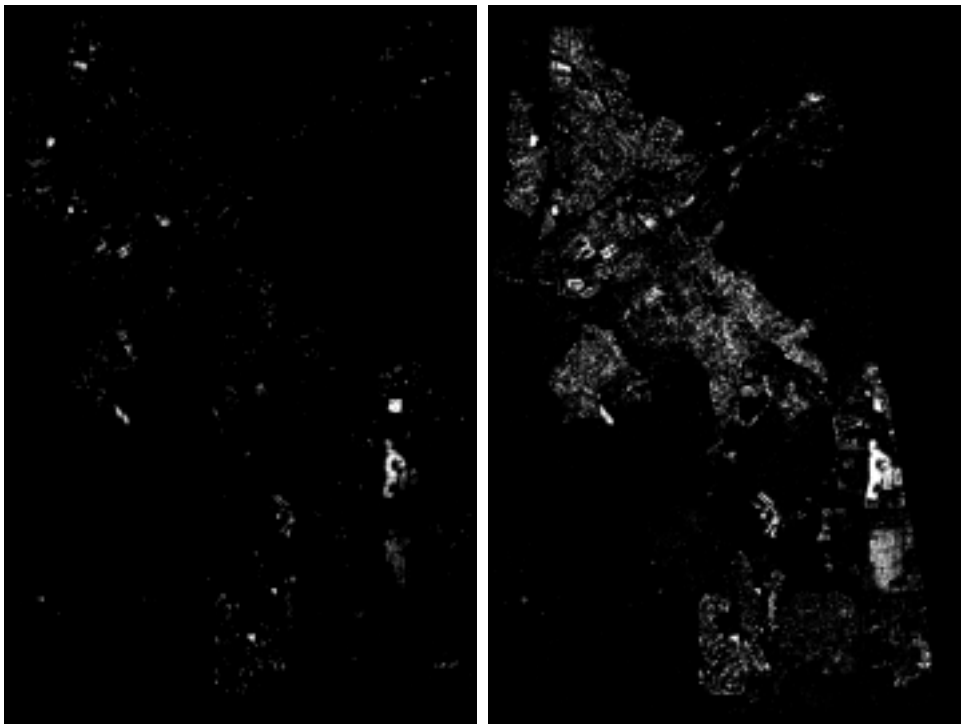

Figure 9: AVIRIS (Left) and MASTER (Right) MTMF mapping results. Grayscale shows abundances for enbmember #3 (Vegetation) scaled to show abundances between 10 and 50% for AVIRIS and between 20 and 100% for MASTER.

4. DISCUSSION AND CONCLUSIONS

Figures 8 and 9 illustrate that use of the AVIRIS spectra modeled to MASTER spectral resolution to map the MASTER data has resulted in similar spatial patterns for specific endmembers. Additionally, Figure 9 demonstrates that at least for some endmembers, MASTER maps significantly more individual pixels at higher abundances than shown by the AVIRIS data – presumably the result of spectral mixing. Using the zoomed comparisons in Figure 10, it is also easy to observe that the MASTER data, as hypothesized, provides additional spatial detail regarding the location of specific endmembers, both in the form of better definition of object shapes and edges, and in the definition of the spatial location of endmembers present only at subpixel abundances in the AVIRIS data. The main achievement of this exercise is the production of an improved-spatial-resolution HSI dataset that incorporates the appropriate HSI spectral signatures at the MSI spatial resolution.

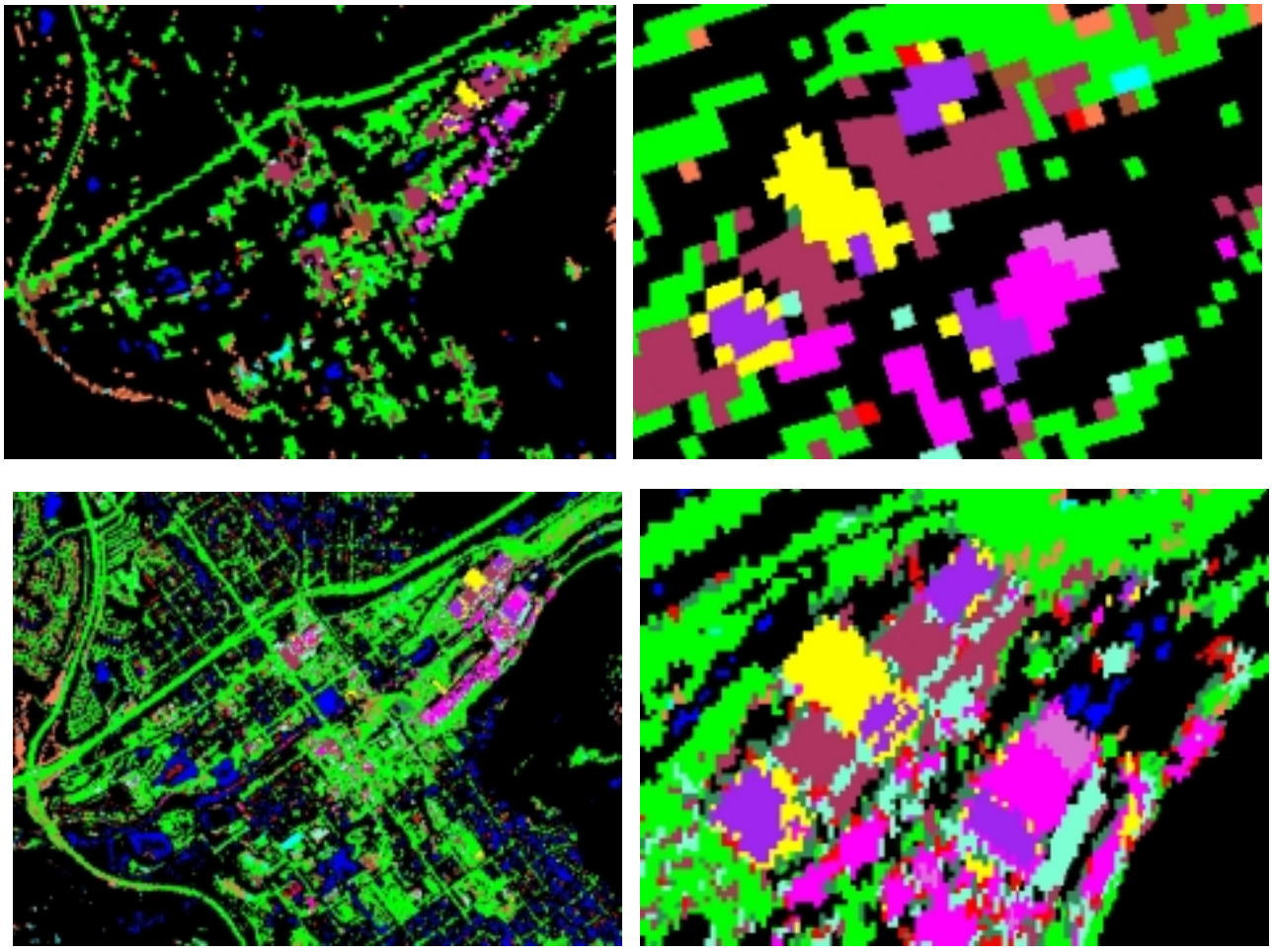

Figure 10: AVIRIS (top) and MASTER (bottom) SAM mapping results. The left images show a portion of the SAM results centered on the city of Golden, Colorado. The right images show the images zoomed by a factor of 4 centered on the Coors Brewery. Classification colors match the colors for endmembers shown in Figure 7.

We believe that the examples shown here validate this approach for spatial/spectral modeling of HSI/MSI data. Further research is required, however, and field verification has yet to be accomplished. While these data are adequate for the purposes of demonstration, there are also significant technical obstacles that need to be overcome, both to fully illustrate the concept and to allow routine use of this approach. These include such factors as:

- Difficulties in obtaining stacked HSI/MSI datasets that are coincident in both space and time (resulting in spatial/spectral changes between datasets)
- Consistent sensor calibration and atmospheric corrections
- Difficulties in locating "pure" (full pixel) spectral signatures in HSI data that are pertinent to higher spatial resolution datasets
- Ambiguities of MSI signatures for materials that are distinctly separable using HSI data
- Problems with georeferencing accuracy along with resampling effects for various spatial scales. A major contribution is required directed at allowing virtual access to multi-resolution datasets without actually performing the intermediate full-image geometric corrections.

Future work should focus on overcoming these technical objectives using a designed experiment. An appropriate site should be identified or constructed with viable, known subpixel targets of interest and near-simultaneous HSI/MSI data should be flown specifically to address this analysis approach. (MSI data should have significantly higher spatial resolution than the HSI data). Supporting ground measurements should be obtained for atmospheric correction and specific ground locations for spatial validation should be predetermined and GPS coordinates collected for use as Ground Control Points (GCPs). Additionally, a second HSI dataset should be flown at the same spatial resolution as the MSI data to be used for verification of the mapping results.

5. REFERENCES

1. Gillespie, A. H., Kahle, A. B. and Walker, R. E., Color Enhancement of Highly Correlated Images. I. Decorrelation and Hue Saturation and Intensity Contrast Stretches: in Remote Sensing of Environment, Vol. 20, pp. 209 – 235, 1986.

2. Lillesand T.M and Kiefer R.W, Remote Sensing and Image Interpretation, Third Edition: John Wiley and Sons Inc., 1994.

3. Vrabel, Jim, Multispectral Imagery Band Sharpening Study, Photogrammetric Engineering & Remote Sensing, Vol. 62, No. 9, pp. 1075-1083, 1996.

4. Winter, M. E., and Winter E. M., Resolution enhancement of hyperspectral data: in Proceedings, 2002 IEEE Aerospace Conference, Big Sky, Montana, 9-16 March 2002 (0n CD-ROM), IEEE Catalog Number 02TH8593C, 2002.

5. Boardman, J. W., and Kruse, F. A., Automated spectral analysis: A geological example using AVIRIS data, northern Grapevine Mountains, Nevada: in Proceedings, Tenth Thematic Conference, Geologic Remote Sensing, 9-12 May 1994, San Antonio, Texas, p. I-407 - I-418, 1994.

6. Kruse, F. A., Boardman, J. W., and Huntington, J. F., Evaluation and Validation of EO-1 Hyperion for Mineral Mapping: in Special Issue, Transactions on Geoscience and Remote Sensing (TGARS), IEEE, v. 41, no. 6, June, p. 1388 – 1400, 2003.

7. Kruse, F. A., Mapping spectral variability of geologic targets using Airborne Visible/Infrared Imaging Spectrometer (AVIRIS) data and a combined spectral feature/unmixing approach: in Proceedings, AeroSense'95, SPIE, 17-21 April 1995, Orlando, Florida, 1995.

8. Boardman, J. W., Kruse, F. A., and Green, R. O., Mapping target signatures via partial unmixing of AVIRIS data: in Summaries, Fifth JPL Airborne Earth Science Workshop, JPL Publication 95-1, 1: 23-26, 1995.

9. Analytical Imaging and Geophysics LLC (AIG), ACORN User's Guide, Stand Alone Version: Analytical Imaging and Geophysics LLC, 64 pp, 2001.

10. Research Systems Inc(RSI), ENVI User's Guide, Research Systems Inc, 1084 p., 2003.

11. Kruse, F. A., Lefkoff, A. B., and Dietz, J. B., Expert System-Based Mineral Mapping in northern Death Valley, California/Nevada using the Airborne Visible/Infrared Imaging Spectrometer (AVIRIS): Remote Sensing of Environment, Special issue on AVIRIS, May-June 1993, v. 44, p. 309 – 336, 1993.

12. Kruse, F. A., Lefkoff, A. B., Boardman, J. B., Heidebrecht, K. B., Shapiro, A. T., Barloon, P. J., and Goetz, A. F. H., The Spectral Image Processing System (SIPS) - Interactive Visualization and Analysis of Imaging Spectrometer Data: Remote Sensing of Environment, Special issue on AVIRIS, May-June 1993, v. 44, p. 145 – 163, 1993.

13. Boardman, J. W., Leveraging the high dimensionality of AVIRIS data for improved subpixel target unmixing and rejection of false positives: mixture tuned matched filtering, in Summaries of the Seventh Annual JPL Airborne Geoscience Workshop, Pasadena, CA, 55 pp, 1998.

14. Porter, W. M., and Enmark, H. E., System overview of the Airborne Visible/Infrared Imaging Spectrometer (AVIRIS), in Proceedings, Society of Photo-Optical Instrumentation Engineers (SPIE), v. 834, p. 22-31, 1987.
15. Green, R. O., M. L. Eastwood, and C. M. Sarture, "Imaging Spectroscopy and the Airborne Visible Infrared Imaging Spectrometer (AVIRIS)," Remote Sens Environ 65: (3) 227–248 SEP 1998.

16. Hook, S. J. Myers, J. J., Thome, K. J., Fitzgerald, M. and A. B. Kahle, The MODIS/ASTER airborne simulator (MASTER) - a new instrument for earth science studies. Remote Sensing of Environment, vol. 76, Issue 1, pp. 93-102, 2001.

17. Roberts, D. A., Yamaguchi, Y., and Lyon, R. J. P., Calibration of Airborne Imaging Spectrometer Data to percent reflectance using field spectral measurements: in Proceedings, Nineteenth International Symposium on Remote Sensing of Environment, Ann Arbor, Michigan, 1985.